Rydberg-Rydberg Collisions: Resonant Enhancement of State Mixing and Penning Ionization

A. Reinhard, T. Cubel Liebisch,* K. C. Younge, P. R. Berman, and G. Raithel

FOCUS Center and Michigan Center for Theoretical Physics, Department of Physics, University of Michigan, Ann Arbor, Michigan 48109, USA

(Received 27 August 2007; revised manuscript received 25 November 2007; published 28 March 2008)

In rubidium Rydberg states, the collision $nD_{5/2} + nD_{5/2} \rightarrow (n-2)F_{7/2} + (n+2)P_{3/2}$ is nearly resonant in the vicinity of $n = 43$. As a result, over a short range of n centered around $n \approx 43$ the Rydberg-Rydberg interaction potential is quite large and turns from repulsive to attractive [Phys. Rev. A **75**, 032712 (2007)]. We use state-selective field ionization to investigate the effect of this resonance on instantaneous excitation of mixed two-particle states, state-mixing collisions, and Penning ionization. We find that these processes depend on the magnitude and sign of the two-particle interaction potential, and thus on n near the resonance. The large magnitude of the observed state mixing provides evidence for many-body effects.

DOI: 10.1103/PhysRevLett.100.123007 PACS numbers: 32.80.Rm, 03.67.−a, 34.20.Cf, 34.50.−s

Rydberg atoms excited from ensembles of laser-cooled ground-state atoms are of interest because they exhibit strong, tunable interactions that lead to excitation blockades [1–3], many-body physics [4–6], state-changing collisions [4,5,7,8], spontaneous evolution to ultracold plasmas [7–11], and the conversion of internal energy to center-of-mass energy [12,13]. Rydberg-Rydberg interactions play an important role in proposed applications such as quantum computation [14,15], quantum cryptography [16], atomic clocks [17], high-precision spectroscopy [15], and mesoscopic entanglement [15]. For such applications, it is important to characterize Rydberg-Rydberg interactions and photoexcitation spectra over a range of quantum numbers. Large ranges of the principal quantum number n in which interaction strengths exhibit a smooth van der Waals scaling behavior ($\propto n^{11}$) stand in contrast with narrow n ranges in which interactions are strongly enhanced and undergo abrupt changes in sign as a result of near-resonant processes. The number and strength of these resonances is different in each Rydberg series nL_J, with given angular momenta L and J. Rydberg interactions in the van der Waals regime [1,2,11] have been investigated. We study the state-mixing and Penning-ionization behavior of Rydberg atoms in the vicinity of a Rydberg-Rydberg collisional resonance. This work differs from complementary research in which an applied electric field was used to tune Rydberg-Rydberg interactions [3–5].

The interaction we study in this Letter,

$$nD_{5/2} + nD_{5/2} \rightarrow (n-2)F_{7/2} + (n+2)P_{3/2}, \quad (1)$$

becomes nearly resonant in Rb at $n = 43$ in zero electric field. The infinite separation energy detuning of this channel, $\Delta = \{W_{(n-2)F_{7/2}} + W_{(n+2)P_{3/2}} - 2W_{nD_{5/2}}\}/h$, increases from -477 to $+208$ MHz in the range $39 \leq n \leq 47$ and crosses zero near $n = 43$ where $\Delta = -8$ MHz (W indicates level energies; quantum defects from [18,19] are used). The interaction potentials near this resonance have been discussed in Ref. [20] (see also Ref. [21]). The dependence of the magnitude and sign of the interaction potential on n near this resonance leads to a clear variation in the observed degrees of resonant state mixing and Penning ionization with n. Our results also indicate that near the resonance we directly excite coherent superpositions of binary Rydberg excitations of the types $|DD\rangle$ and $(1/\sqrt{2})(|PF\rangle + |FP\rangle)$. Further, we measure a fraction of atoms in P and F states that is significantly larger than that predicted by a binary collision model; these results suggest that many-body effects play an important role in our system [4,5].

We cool and trap ^{85}Rb atoms in a magneto-optical trap (MOT) with full diameter of ~ 300 μm. The MOT densities and atom numbers are $\sim 1.2 \times 10^{10}$ cm^{-3} and $\sim 1.3 \times 10^6$, as determined by shadow imaging. We prepare atoms in nD and nS Rydberg states using two-photon excitation ($5S_{1/2} \rightarrow 5P_{3/2}$; $5P_{3/2} \rightarrow nD, nS$), implemented by turning off the MOT trapping light 10 μs before excitation and applying two coincident, counterpropagating, narrow-linewidth, resonant laser pulses. The upper transition pulse is focused into the MOT with an intensity profile FWHM of 12 μm $\pm$ 1 μm. We excite atoms into a given Rydberg state and determine the state distribution after a variable interaction time using state-selective field ionization (SSFI) with a microchannel-plate detector. The uncertainty in the delay between excitation and SSFI is 50 ns. Further details on the experimental system can be found in Ref. [2].

SSFI electron signals for excitation into $43D_{3/2}$, $43D_{5/2}$, and $45S$ states are shown in Fig. 1 along with the field-ionization electric-field pulse. The excitation pulses have a linewidth <5 MHz and FWHM intensity duration of 100 ns. The field-ionization pulses are applied 200 ns after excitation. Under these conditions, atomic motion is negligible and any state mixing occurs on a fairly rapid time scale (<300 ns). The SSFI spectra compared in Fig. 1 correspond to states with approximately the same effective principal quantum numbers, $n^* = n - \delta_\ell$ ($\delta_S = 3.13$ and $\delta_D = 1.35$ [18]), and hence ionize at roughly the same electric field, $F = -1/(16n^{*4})$. In Fig. 1, we highlight three regions of the electron signal, labeled A, B, and C.

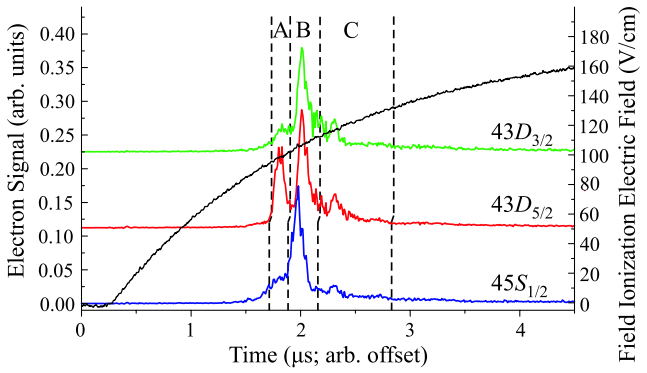

FIG. 1 (color online). Electron signals (left axis) for excitation into $43D_{3/2}$, $43D_{5/2}$, and $45S_{1/2}$ Rydberg states and the SSFI electric-field pulse (right axis). Regions A, B, and C correspond to Rydberg atoms populated by direct photoexcitation (B) and combined photoexcitation-collisional processes (A, C).

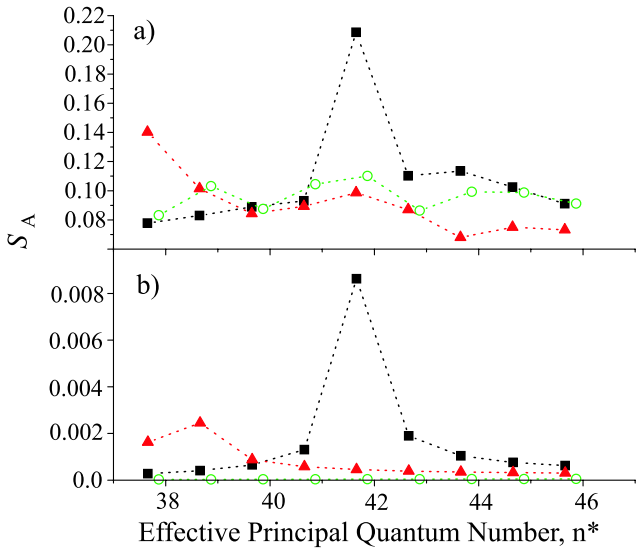

FIG. 2 (color online). S_A as a function of the effective principal quantum number of the states into which the atoms are excited. Results are shown for $D_{5/2}$ (squares), $D_{3/2}$ (triangles), and S (circles) states. (a) Experiment and (b) theory.

These regions correspond to the ionization electric-field ranges of Rydberg atoms with effective principal quantum numbers $n^* \in]42, 43[$, $n^* \in]41, 42[$, and $n^* \in]40, 41[$, respectively. Population in regions A and C is generated as a result of the type of interaction indicated in Eq. (1).

Figure 1 provides evidence for qualitative differences in the state-mixing behavior of different quantum states of approximately equal energy. The $43D_{5/2}$ state, detected in region B, is characterized by significant mixing to $45P$ and $41F$ states, detected in regions A and C, respectively. The $43D_{3/2}$ and $45S$ states, both detected in region B, exhibit much less mixing, owing to the absence of any near-resonant channel for these states.

For laser excitation into $D_{5/2}$ or $D_{3/2}$ states, the nearest-resonant interaction channels involve transitions into higher-lying P and lower-lying F states, as in Eq. (1), while for excitation into $S_{1/2}$ states all interaction channels only involve transitions into P states. In all cases shown in Fig. 1, a quantitative measure for the amount of mixing into higher-lying P states is given by S_A, the integral of the electron signal detected in region A divided by the total integral. Similarly, mixing into lower-lying states can be quantified via S_C, the integral of the signal in region C divided by the total integral. Here, we choose to analyze the value of S_A rather than S_C because P-Rydberg states, which make up most of the signal detected in A, ionize over a narrower electric-field range than F states, which in most cases are the dominant signal detected in C. In Fig. 2(a), we show experimental values of S_A as a function of n^* for $D_{3/2}$, $D_{5/2}$, and S states [22]. Evaluating S_A for several choices for the integration boundaries that separate regions A, B, and C, we determine that the uncertainty of experimental S_A values ranges from about 0.005 to 0.03, depending on the initially excited Rydberg state. The data in Fig. 2(b) show calculated fractions of Rydberg-state populations in higher-lying P states (discussed below).

The curve in Fig. 2(a) for $nD_{5/2}$ states is characterized by a strong enhancement of the mixing at $n^* = 41.65$, where $S_A \approx 0.21$. This observation reflects the fact that the channel in Eq. (1) becomes nearly resonant at $n = 43$. To interpret this result, we first note that the SSFI peaks in Fig. 1 overlap somewhat with one another. The integral over region A therefore includes some atoms that actually belong to the B peak. This error results in a fairly constant background of S_A of ≈ 0.09. Because of the background, we assume the peak value of S_A of 0.21 corresponds to an actual fraction of atoms in $P_{3/2}$ product states of only ≈ 0.12. We have verified that saturation caused by temporal overlap of microchannel-plate pulses does not significantly alter the S_A values. We conclude that for the conditions of Fig. 2(a) the near resonance of the channel in Eq. (1) at $n = 43$ causes a transfer of up to about 12% of the excited atoms into P states. This transfer occurs almost instantaneously because of the short duration of the excitation pulses and the almost instantaneous detection.

Inspection of the curve for $nD_{3/2}$ in Fig. 2(a) shows that in the range $n^* < 40$ the S_A value increases from the background level of ≈ 0.09 to ≈ 0.14. This rise reflects another, relatively weak, near-resonant interaction identified in Ref. [20], namely $2 \times 39D_{3/2} \rightarrow 37F_{5/2} + 41P_{3/2}$. Otherwise, the S_A values in Fig. 2(a) largely remain at the background level, in accordance with the absence of any other near-resonant collision channels.

To model the results in Fig. 2(a), we numerically solve the full density matrix equations (including decay from the $5P_{3/2}$ state) in the two-particle space $\{|ss\rangle, |pp\rangle, |dd\rangle, \frac{1}{\sqrt{2}}(|sp\rangle + |ps\rangle), \frac{1}{\sqrt{2}}(|sd\rangle + |ds\rangle), \frac{1}{\sqrt{2}}(|pd\rangle + |dp\rangle), \frac{1}{\sqrt{2}}(|p'f\rangle + |fp'\rangle), \frac{1}{\sqrt{2}}(|sp\rangle - |ps\rangle), \frac{1}{\sqrt{2}}(|sd\rangle - |ds\rangle), \frac{1}{\sqrt{2}}(|pd\rangle - |dp\rangle)\}$, assuming binary interactions and negligible atomic motion. The single-atom states $|s\rangle$, $|p\rangle$, $|d\rangle$,

$|p'\rangle$, and $|f\rangle$ correspond to the $5S_{1/2}$, $5P_{3/2}$, $nD_{5/2}$, $(n+2)P_{3/2}$, and $(n-2)F_{7/2}$ states. The excitation is modeled by two coincident Gaussian laser pulses with an intensity FWHM of 100 ns that resonantly couple $|s\rangle$ to $|p\rangle$ and $|p\rangle$ to $|d\rangle$. In the simulation, the peak Rabi frequency of the lower transition is 3.5 MHz, as calculated from experimental Autler-Townes splitting data [23], and that of the upper transition is estimated to be 3 MHz. For a range of the dipole-dipole coupling strength V_{dd} of the channel in Eq. (1), $h \times 1$ MHz $\leq V_{dd} \leq h \times 25$ MHz, we solve the master equations and extract the fraction of atoms in the $|p'\rangle$ state 200 ns after excitation. The $|p'\rangle$ fractions have a maximum within this range of V_{dd}, shown as squares in Fig. 2(b) as a function of n. Using appropriate sets of different basis states, energy detunings, and coupling strengths, analogous results are also obtained for $nD_{3/2}$ and nS states [triangles and circles in Fig. 2(b)].

The model is quite successful in reproducing all qualitative features of Fig. 2(a), but the experimental values of S_A are about 14 times larger than the theoretical values. Several factors may cause disagreement between the experimental and calculated values of S_A. We find that S_A is sensitive to several parameters which are not precisely known, including the upper-transition Rabi frequency and the energy detuning of the channel in Eq. (1). In our calculations, we also neglect the magnetic substructure of the atoms. Most importantly, we neglect excitations involving more than two particles. Theoretical work in progress incorporates more than two atoms as well as "state-swapping" couplings between pairs of interacting atoms and background Rydberg atoms. For example, the $|p'\rangle$ fraction can be increased a factor of 2 or more for a wide range of three-particle configurations. Thus, we believe that inclusion of more than three atoms will lead to substantially better quantitative agreement between theory and experiment.

In the results shown so far, the time between excitation and detection has been fixed at 200 ns, which is sufficiently short to ensure that the atoms remain fixed in space. In the following discussion, we explore time-delayed collisions, which may be triggered by the effect of interatomic forces on the atomic motion [10,11]. In Fig. 3 we show the S_A fraction measured as a function of the time delay between excitation and detection for $41D_{5/2}$, $43D_{5/2}$, and $45D_{5/2}$ states. Within 200 ns of excitation, the S_A value measured for excitation to $43D_{5/2}$ reaches ≈ 0.18. This is somewhat lower than the corresponding value in Fig. 2(a), presumably because of experimental variations in atom density. As the time delay is increased, the S_A value increases to a steady state of ≈ 0.24 within several microseconds. For excitation into $45D_{5/2}$, a qualitatively similar behavior is observed, with S_A values being ≈ 0.03 lower than for excitation into $43D_{5/2}$. In contrast, for excitation into $41D_{5/2}$ states much lower S_A values are measured, and S_A does not increase as a function of the excitation-probe delay time.

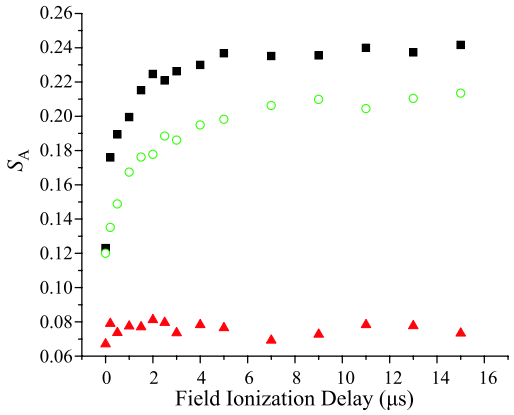

FIG. 3 (color online). S_A as a function of the delay between excitation and field ionization for excitation into $41D_{5/2}$ (triangles), $43D_{5/2}$ (squares), and $45D_{5/2}$ (circles) states.

The resonance of the channel in Eq. (1) at $n = 43$ leads to enhanced attractive interaction for several n states above $n = 43$ and repulsive interaction for several n states below $n = 43$ [20]. Atoms excited on a repulsive potential will not move together whereas atoms on an attractive potential will move together, form mixed quantum states, and may eventually ionize [8]. In the case of $45D_{5/2}$ in Fig. 3, in which the channel in Eq. (1) is attractive, the S_A value rapidly increases with field-ionization delay within a few microseconds. We believe that this increase is due to additional state mixing produced in time-delayed collisions triggered by attractive interatomic forces. In the case $41D_{5/2}$, in which the interaction is weak and repulsive, the S_A value remains constant as a function of field-ionization delay. This observation is consistent with the absence of additional state mixing produced in time-delayed collisions. In the case $43D_{5/2}$ the detuning Δ is of the same order as the excitation bandwidth, leading to the creation of atom pairs on both attractive and repulsive molecular potentials. This may explain why the data for $43D_{5/2}$ exhibit both an almost instantaneous initial rise and a time-delayed, gradual increase in S_A.

In Fig. 4 we show the value of S_A as a function of the field-ionization delay for several different angular momentum states of approximately equal n^* ($43D_{3/2}$, $43D_{5/2}$, and $45S$). We observe that for $43D_{5/2}$ states the S_A value increases much more rapidly and reaches a much higher steady-state value than for the $43D_{3/2}$ and $45S$ states. We attribute this behavior to the fact that the $43D_{5/2}$ state exhibits a strong, near-resonant interaction [Eq. (1)] while the other two states do not.

The resonance of the interaction channel in Eq. (1) at $n = 43$ affects not only the state-mixing dynamics of $nD_{5/2}$ Rydberg atoms, but also Penning ionization. To investigate ionization, we excite Rydberg atoms with 500 ns laser pulses and measure the number of free electrons generated. In our data, free electrons produce a peak at the onset of the SSFI pulse. To quantify ionization, we

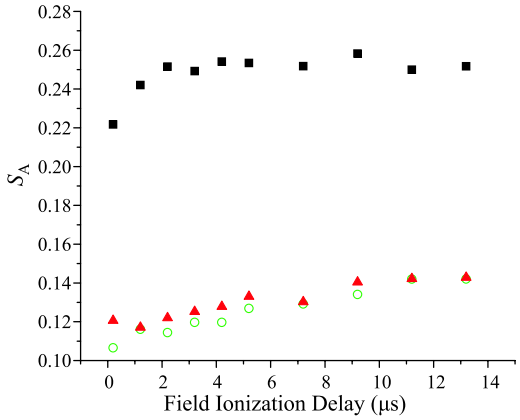

FIG. 4 (color online). S_A as a function of the time delay between excitation and field ionization for excitation into $43D_{3/2}$ (circles), $43D_{5/2}$ (squares), and $45S$ (triangles) states.

define the Penning-ionization probability S_{FE} as the integral of the free-electron peak divided by the total integral of the electron signal. Figure 5(a) shows that S_{FE} approaches a steady-state after a few tens of microseconds of evolution. In Fig. 5(b) we show S_{FE} for $nD_{5/2}$ states after 15 μs interaction time as a function of n. S_{FE} is approximately constant at $\sim$0.10, except for a drop in the range $n = 41$–43 and a moderate elevation at $n = 40$. We attribute the drop in the range $n = 41$–43 to a reduction in collisions due to the repulsive interactions between Rydberg atoms expected in that range of n [20]. While the elevation at $n = 40$ is not fully understood, we note that, following Ref. [20], Rb atoms in state $40D_{5/2}$ exhibit relatively weak interaction due to an accidental cancellation of the level-shift contributions associated with several interaction channels. The weak interaction at $n = 40$ is expected to weaken the Rydberg excitation blockade and to lead to a relatively large fraction of Rydberg-atom pairs at close distances, which may cause enhanced ionization. Overall, the interaction channel in Eq. (1) plays a significantly smaller role in Penning ionization than it does in the

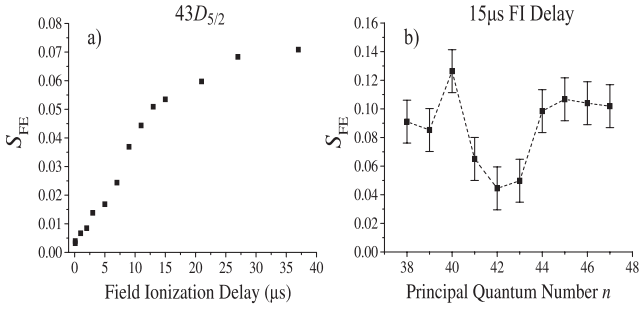

FIG. 5. (a) Penning-ionization probability S_{FE} for $43D_{5/2}$ as a function of field-ionization delay. (b) S_{FE} for $nD_{5/2}$ states as a function of n after 15 μs field-ionization delay. The data are taken using cold atom clouds with a diameter of about 35 μm and a peak density of order 5×10^{10} cm^{-3}, prepared in an optical dipole trap.

near-resonant state-mixing collisions discussed earlier. This may be because Penning ionization is a deep, inelastic process, which should depend less on a single, near-elastic interaction channel than the state mixing studied in this work.

In conclusion, we have shown that the probabilities for resonant state-changing and Penning-ionizing collisions of Rb Rydberg atoms depend sensitively on the magnitude and sign of the interaction energy, and thus on n in the vicinity of a collisional resonance. Direct evidence is provided for the abrupt change in magnitude and sign of the Rydberg-Rydberg interactions near $43D_{5/2}$ due to the channel in Eq. (1). We have found unexpectedly large amounts of state mixing near this resonance. In calculations, we have obtained preliminary evidence that the state mixing is strongly enhanced by many-body effects. In the future, one may study state mixing and Penning ionization near this resonance as a function of density in order to probe for such many-body physics.

The authors acknowledge fruitful correspondence with T. Pohl. This work was supported in part by NSF Grants No. PHY-0114336, No. PHY-0555520, and No. PHY-0244841.

*Present address: NIST Time and Frequency Division, 325 Broadway, Boulder, CO 80305, USA.

[1] D. Tong *et al.*, Phys. Rev. Lett. **93**, 063001 (2004).
[2] T. Cubel Liebisch *et al.*, Phys. Rev. Lett. **95**, 253002 (2005).
[3] T. Vogt *et al.*, Phys. Rev. Lett. **97**, 083003 (2006).
[4] W. R. Anderson *et al.*, Phys. Rev. Lett. **80**, 249 (1998).
[5] I. Mourachko *et al.*, Phys. Rev. Lett. **80**, 253 (1998).
[6] T. J. Carroll *et al.*, Phys. Rev. A **73**, 032725 (2006).
[7] A. Walz-Flannigan *et al.*, Phys. Rev. A **69**, 063405 (2004).
[8] W. Li *et al.*, Phys. Rev. A **70**, 042713 (2004).
[9] M. P. Robinson *et al.*, Phys. Rev. Lett. **85**, 4466 (2000).
[10] W. Li *et al.*, Phys. Rev. Lett. **94**, 173001 (2005).
[11] T. Amthor *et al.*, Phys. Rev. Lett. **98**, 023004 (2007).
[12] F. Robicheaux, J. Phys. B **38**, S333 (2005).
[13] B. Knuffman and G. Raithel, Phys. Rev. A **73**, 020704(R) (2006).
[14] D. Jaksch *et al.*, Phys. Rev. Lett. **85**, 2208 (2000).
[15] M. D. Lukin *et al.*, Phys. Rev. Lett. **87**, 037901 (2001).
[16] M. Saffman and T. G. Walker, Phys. Rev. A **66**, 065403 (2002).
[17] I. Bouchoule and K. Mølmer, Phys. Rev. A **65**, 041803 (2002).
[18] W. Li *et al.*, Phys. Rev. A **67**, 052502 (2003).
[19] J. Han *et al.*, Phys. Rev. A **74**, 054502 (2006).
[20] A. Reinhard *et al.*, Phys. Rev. A **75**, 032712 (2007).
[21] Older sets of quantum defects, used in Ref. [20], produce values of Δ different than these values by approximately tens of MHz.
[22] Whenever n, ℓ, or j is varied, the upper-transition Rabi frequency is kept constant by adjusting the laser intensity by an appropriate scale factor.
[23] B. K. Teo *et al.*, Phys. Rev. A **68**, 053407 (2003).